

# Orbital order-disorder transition with volume collapse in $\text{HoBaCo}_2\text{O}_{5.5}$ : A high-resolution neutron diffraction study

E. Pomjakushina,<sup>1,2,\*</sup> K. Conder,<sup>1</sup> and V. Pomjakushin<sup>2</sup><sup>1</sup>Laboratory for Developments and Methods, PSI, 5232 Villigen, Switzerland<sup>2</sup>Laboratory for Neutron Scattering, ETHZ & PSI, 5232 Villigen, Switzerland

(Received 23 November 2005; published 13 March 2006)

The crystal structure of the layered cobaltite  $\text{HoBaCo}_2\text{O}_{5.5}$  (substituted with both  $^{16}\text{O}$  and  $^{18}\text{O}$ ) was studied across an insulator to metal (MI) transition at  $T_{\text{MI}}=305$  K employing high-resolution neutron diffraction. We have found that the transition at  $T_{\text{MI}}$  is of the first-order type, accompanied by an abrupt negative change of the unit cell volume ( $\sim 0.15\%$ ) and melting of the orbital order in the pyramids. The existence of an isotope effect on  $T_{\text{MI}}$  suggests that the structure changes are caused by the electron delocalization above the transition.

DOI: 10.1103/PhysRevB.73.113105

PACS number(s): 71.30.+h, 71.70.Ej, 64.60.Cn, 61.12.Ld

The layered perovskite  $\text{R}\text{BaCo}_2\text{O}_{5+\delta}$  (where  $R$  is a rare earth element) family possesses extremely rich structural, electronic, and magnetic phase diagrams due to the strong coupling between charge, orbital, and spin degrees of freedom. Since cobalt cations in this system can adopt different oxidation states, the oxygen content can be varied in a very wide range ( $0 < \delta < 1$ ). In the  $\text{R}\text{BaCo}_2\text{O}_{5.5}$  structure, the cobalt cations occupy two crystallographic sites with different coordination environments—pyramidal  $\text{CoO}_5$  and octahedral  $\text{CoO}_6$ . The presence of Co in the +3 oxidation state (electron configuration  $3d^6$ ) leads to a Jahn-Teller distortion of the oxygen octahedra in the orthorhombic structure ( $Pmmm$  space group). The spin state of the  $\text{Co}^{3+}$  ion can vary from low spin (LS) ( $S=0$ ) to high spin (HS) ( $S=3$ ) and the change can be triggered, e.g., by temperature. This spin transition in  $\text{LaBaCo}_2\text{O}_{5.5}$  is believed to be coupled to the metal-insulator (MI) transition,<sup>1–9</sup> at which electrons transfer from localized states to collective states at temperatures above  $T_{\text{MI}}$ . Due to the strong spin-orbital coupling the crystal structure undergoes pronounced changes at the transition. To elucidate the mechanism of the MI transition, the temperature changes of the crystal structure at the  $T_{\text{MI}}$  were studied in several papers.<sup>11–13</sup> In  $\text{YBaCo}_2\text{O}_{5+\delta}$  ( $0.50 \leq \delta$ ) this transition was accompanied by a large lattice distortion<sup>11</sup> and a phase separation was proposed to be concomitant with the charge order transition. In  $\text{TbBaCo}_2\text{O}_{5+\delta}$  ( $\delta=0.5$ ), showing a metal-

insulator transition at  $T_{\text{MI}}=340$  K, it was found that both pyramids and octahedra are significantly distorted below  $T_{\text{MI}}$ ; thus a  $d_{3x^2-r^2}/d_{3y^2-r^2}$  orbital ordering (OO) transition was suggested.<sup>12</sup> Opposite to the above finding,<sup>12</sup> the proposed driving force for the MI transition in  $\text{GdBaCo}_2\text{O}_{5.5}$  is only the spin-state switch in  $\text{Co}^{3+}$  ions located at the octahedra, completely excluding the orbital ordering effects.<sup>13</sup>

We have undertaken a high-resolution neutron diffraction measurements of the crystal structure across the MI transition in  $\text{HoBaCo}_2\text{O}_{5.5}$ .  $\text{HoBaCo}_2\text{O}_{5+\delta}$  has been chosen because for this compound the annealing conditions used for the oxygen isotope substitution give the equilibrium oxygen content very close to 5.5. The present work presents the crystal structure parameters in both  $^{16}\text{O}$ - and  $^{18}\text{O}$ -substituted samples and complements our work on the oxygen isotope effect on the transition temperature  $T_{\text{MI}}$  in the series of  $\text{R}\text{BaCo}_2\text{O}_{5.5}$  ( $R=\text{Pr, Dy, Ho, and Y}$ ).<sup>15</sup>

The initial  $\text{HoBaCo}_2\text{O}_{5+\delta}$  was synthesized by a solid state reaction using  $\text{Ho}_2\text{O}_3$ ,  $\text{BaCO}_3$ , and  $\text{Co}_3\text{O}_4$  of a minimum purity of 99.99%. The details of the synthesis procedure, oxygen isotope exchange, and oxygen content determination have been given previously.<sup>10,15</sup> The oxygen content amounts to  $5.46 \pm 0.01$ . Differential scanning calorimetry (DSC) was used for the determination of the MI transition temperature, as it was previously applied in nickelates<sup>14</sup> and cobaltates.<sup>11,15</sup> The transition temperatures and enthalpies in the studied samples (see Fig. 1), were  $T_{\text{MI}}=303.3$  and

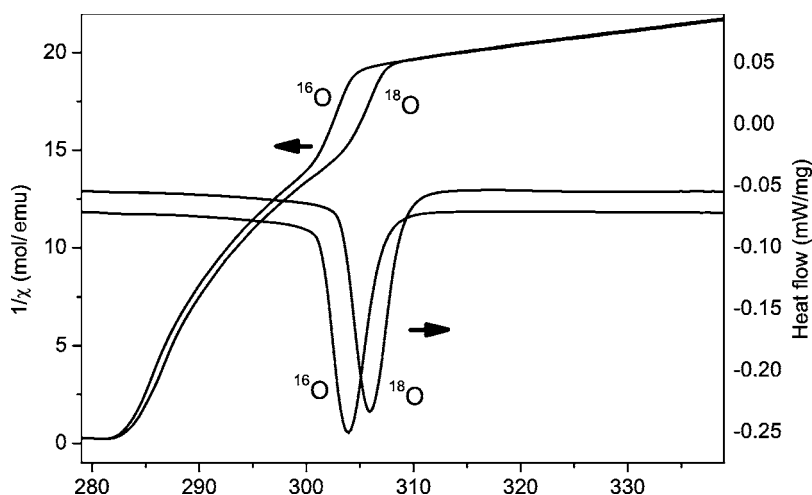


FIG. 1. Temperature dependencies of inverse magnetic susceptibility and DSC signal for  $^{16}\text{O}$ - and  $^{18}\text{O}$ -substituted samples.

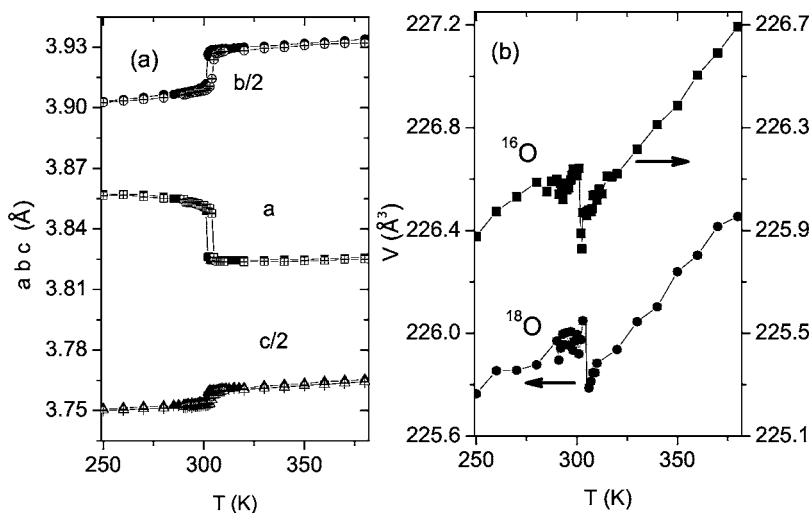


FIG. 2. Temperature dependence of (a) crystal lattice constants (open symbols are for  $^{18}\text{O}$ -substituted sample); (b) unit cell volume for  $^{16}\text{O}$ - and  $^{18}\text{O}$ -substituted samples.

305.2 K and 4.48(13) and 4.50(5) kJ/mol for the  $^{16}\text{O}$  and  $^{18}\text{O}$  samples, respectively. It was shown before<sup>15</sup> that the DSC peak position as well as the peak area (transition enthalpy) are very sensitive to the oxygen content. The equality of the MI transition enthalpies in our samples provides evidence for a practically identical oxygen content, in agreement with iodometric titration. The magnetic susceptibility measurements have shown that the transition is accompanied by an abrupt change in the slope of the inverse susceptibility (Fig. 1) implying a change of the Co spin state, similarly to those observed previously.<sup>13</sup>

Neutron powder diffraction measurements were carried out at the high-resolution HRPT diffractometer<sup>16</sup> at SINQ neutron spallation source (PSI, Switzerland). The high-intensity mode of HRPT was used with the neutron wavelength  $\lambda = 1.49$  Å. The refinements of the crystal structure parameters were performed using the FULLPROF program,<sup>17</sup> with the use of its internal tables for neutron scattering lengths.

Figure 2(a) shows the temperature dependence of the lattice constants of  $\text{HoBaCo}_2\text{O}_{5.5}$ . Whereas the observed crystal symmetry was orthorhombic ( $Pmmm$ ) in the whole investigated temperature range, the lattice constants undergo dramatic changes. With an increase in temperature both  $b$  and  $c$  parameters show sharp positive jumps of +0.7% and +0.3%, respectively at  $T_{MI} = 305$  K. At the same temperature the  $a$  parameter drops by -0.3%. These anisotropic changes of the crystal unit cell result in an abrupt negative drop (-0.15%) of the unit cell volume  $V$  at  $T_{MI}$  [see Fig. 2(b)]. This finding and the observation of the latent heat by DSC indicate that the transition is of a first-order type. The drop and back relaxing of the unit cell volume take place within a very narrow temperature interval of about 3 K. This effect was not detected before<sup>11–13</sup> probably because the temperature scans have been done with rather big temperature steps. In a narrow temperature interval ( $\approx 2$  K) in the vicinity of  $T_{MI}$ , a coexistence of the low- and high-temperature structures has been clearly observed in the diffraction data, providing additional evidence for the first-order type of transition. A contraction of the unit cell volume at the insulator to metal transition is a usual feature in manganites and cobaltates, reflecting the delocalization of the charge carriers. A similar

volume collapse effect (-0.5%) was observed at the orbital order-disorder transition in  $\text{LaMnO}_3$ ,<sup>18</sup> also accompanied by appearance of a conductive phase.<sup>19</sup>

The temperature behavior of all the structure parameters in both  $^{16}\text{O}$  and  $^{18}\text{O}$  samples is qualitatively the same as the shift of the transition temperature as already shown in Fig. 2. However, for completeness we present the results for both  $^{16}\text{O}$ - and  $^{18}\text{O}$ -substituted samples in some figures. The temperature dependence of the bond lengths in  $\text{CoO}_5$  pyramids and  $\text{CoO}_6$  octahedra is shown in Figs. 3 and 4, respectively. Figure 5 presents the schematic crystal structure of  $\text{HoBaCo}_2\text{O}_{5.5}$  at temperatures below and above the MI transition. In Fig. 5 the differences in the atomic positions caused by the MI transition are rescaled to larger values for better visibility. In the high-temperature phase all the  $\text{Co2-O}$  bond distances [ $\text{Co2-O4}$  ( $a$ ),  $\text{Co2-O6}$  ( $b$ ), and  $\text{Co2-O1}$  ( $c$ )] become equal, and consequently the  $\text{CoO}_5$  pyramids are regular above the transition (see Fig. 3). In contrast, in the  $\text{CoO}_6$  octahedra the bond distances along the  $c$  direction, i.e.,  $\text{Co1-O2}$  and  $\text{Co1-O3}$ , become different in the high-

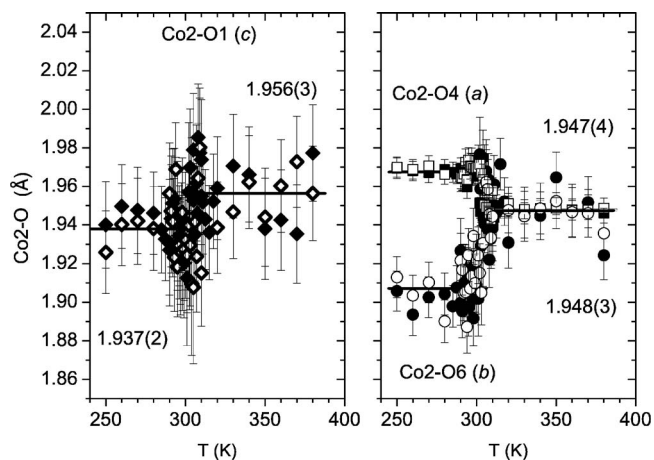


FIG. 3. Temperature dependence of  $\text{Co2-O}$  bond lengths in  $\text{CoO}_5$  pyramids:  $\text{Co2-O1}$  ( $c$ ),  $\text{Co2-O4}$  ( $a$ ),  $\text{Co2-O6}$  ( $b$ ). The letters  $a, b, c$  indicate the approximate direction of the bonds with respect to the crystal axes. Lines are the linear fits above and below the transition with the refined values of the bond lengths indicated. The open and closed symbols represent the  $^{18}\text{O}$  and  $^{16}\text{O}$  samples.

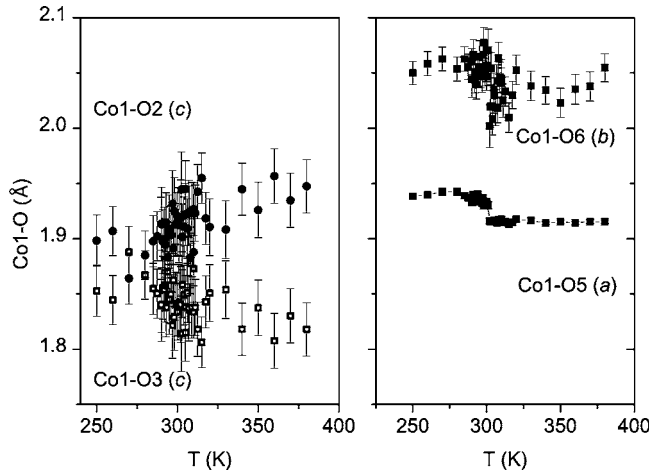


FIG. 4. Temperature dependence of Co1-O bond lengths in  $\text{CoO}_6$  octahedra: Co1-O2 (c), Co1-O3 (c), Co1-O6 (b), Co1-O5 (a). The letters *a, b, c* indicate the approximate direction of the bonds with respect to the crystal axes.

temperature phase, whereas in-plane bond lengths (Co1-O6 and Co1-O5) are almost unaffected by the transition. Results shown in Figs. 3 and 4 suggest an orbital ordering in the (*ab*) plane below  $T_{\text{MI}}$ . The bond lengths in the *ab* plane are significantly different, implying that the  $d_{3x^2-r^2}$  orbitals are ordered similarly, as has been proposed.<sup>12</sup> The OO expands over all Co ions in both octahedral (Co1) and pyramidal (Co2) surroundings, i.e., the longest bond length Co1-O6 matches the shortest Co2-O6 (see also Fig. 5). Above  $T_{\text{MI}}$  the OO in the pyramids completely disappears, as is clearly seen from Fig. 3.

The OO transition can originate from the delocalization of the electrons on the pseudocubic  $e_g$  orbitals in the one-dimensional Co2 pyramid network. Unlike the case of  $\text{TbBaCo}_2\text{O}_{5.5}$ ,<sup>12</sup> the in-plane bond lengths of the Co1 in the octahedra do not become equal above  $T_{\text{MI}}$ . However, both angles  $\varphi$  between octahedra Co1-O5-Co1 and between pyramids Co2-O4-Co2 are increased at the transition temperature

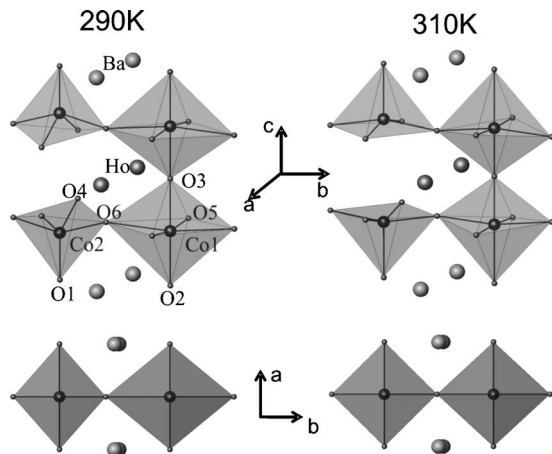


FIG. 5. A schematic crystal structure of  $\text{HoBaCo}_2\text{O}_{5.5}$  at temperatures below (290 K) and above (310 K) the MI transition. The differences in the atomic positions caused by the MI transition are rescaled to larger values for better visibility.

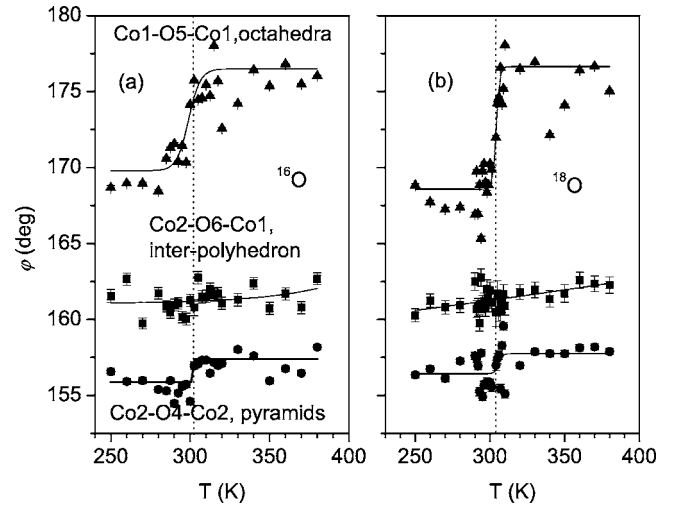


FIG. 6. Temperature dependence of the angles  $\varphi$  between octahedra Co1-O5-Co1, pyramids Co2-O4-Co2, and interpolyhedron Co2-O6-Co1 for  $^{16}\text{O}$ - (a) and  $^{18}\text{O}$ - (b) substituted samples.

(Fig. 6), implying that the electron transfer integral through Co-O-Co, which is proportional to  $\sim \cos(\pi - \varphi)$ , has a step-like increase, suggesting that the electron delocalization occurs in all directions. The transfer integral  $t$  can be renormalized due to the electron-phonon coupling in the small polaron theory  $t \sim t_0 \exp(-\gamma E / \hbar \omega)$ , where  $\omega$  is the optical phonon frequency and  $E$  the polaron binding energy. Since the narrowing is greater for heavier oxygen mass one expects an increase in the transition temperature as proposed before for nickelates<sup>14</sup> and discussed for the present system.<sup>15</sup> Another explanation of the OO transition would be a change of the spin state of the Co2 ions in pyramids. This type of effect was concluded to be present in  $\text{GdBaCo}_2\text{O}_{5.5}$ ,<sup>13</sup> where the spin-state transition of Co ions from LS to HS was proposed to occur solely in the octahedra. The inverse susceptibility  $\chi^{-1}(T)$  in our case (see Fig. 1) also reveals a sharp transformation coinciding with  $T_{\text{MI}}$  for both  $^{16}\text{O}$ - and  $^{18}\text{O}$ -substituted samples.<sup>15</sup> The spin transition to the HS state in the pyramids could also result in the equalizing of the bond lengths. However, this spin-switch type of transition is not expected to have the observed isotope effect.

In conclusion, we presented the temperature dependence of the structure parameters in  $\text{HoBaCo}_2\text{O}_{5.5}$  determined by means of high-resolution neutron diffraction at temperatures 250–400 K. We have shown that the insulator to metal transition above  $T_{\text{MI}}=305$  K occurs concomitantly with the melting of the orbital order in pyramids and increase of the Co-O-Co bond angle together with unit cell volume collapse. The positive isotope exponent on  $T_{\text{MI}}$  supports the idea that the observed structure changes are caused by electron delocalization above the transition.

We acknowledge the allocation of urgent beam time at the HRPT diffractometer of the Laboratory for Neutron Scattering (ETHZ & PSI, Switzerland). The authors thank NCCR MaNEP project for support of this study. The work was partially performed at the neutron spallation source SINQ.

\*Electronic address: ekaterina.pomjakushina@psi.ch

- <sup>1</sup>C. Martin, A. Maignan, D. Pelloquin, N. Nguyen, and B. Raveau, *Appl. Phys. Lett.* **71**, 1421 (1997).
- <sup>2</sup>F. Fauth, E. Suard, V. Caignaert, and I. Mirebeau, *Phys. Rev. B* **66**, 184421 (2002).
- <sup>3</sup>A. Maignan, C. Martin, D. Pelloquin, N. Nguyen, and B. Raveau, *J. Solid State Chem.* **142**, 247 (1999).
- <sup>4</sup>H. Kusuya, A. Machida, Y. Moritomo, K. Kato, E. Nishibori, M. Takata, M. Sakata, and A. Nakamura, *J. Phys. Soc. Jpn.* **70**, 3577 (2001).
- <sup>5</sup>A. Maignan, V. Caignaert, B. Raveau, D. Khomskii, and G. Sawatzky, *Phys. Rev. Lett.* **93**, 026401 (2004).
- <sup>6</sup>M. Respaud, C. Frontera, J. L. García-Muñoz, Miguel Angel G. Aranda, B. Raquet, J. M. Broto, H. Rakoto, M. Goiran, A. Llobet, and J. Rodríguez-Carvajal, *Phys. Rev. B* **64**, 214401 (2001).
- <sup>7</sup>S. Roy, M. Khan, Y. Q. Guo, J. Craig, and N. Ali, *Phys. Rev. B* **65**, 064437 (2002).
- <sup>8</sup>M. Soda, Y. Yasui, M. Ito, S. Iikubo, M. Sato, and K. Kakurai, *J. Phys. Soc. Jpn.* **73**, 4649 (2004).
- <sup>9</sup>A. A. Taskin, A. N. Lavrov, and Y. Ando, *Phys. Rev. B* **71**, 134414 (2005).
- <sup>10</sup>K. Conder, E. Pomjakushina, A. Soldatov, and E. Mitberg, *Mater. Res. Bull.* **40**, 257 (2005).
- <sup>11</sup>D. Akahoshi and Y. Ueda, *J. Solid State Chem.* **156**, 355 (2001).
- <sup>12</sup>Y. Moritomo, T. Akimoto, M. Takeo, A. Machida, E. Nishibori, M. Takata, M. Sakata, K. Ohoyama, and A. Nakamura, *Phys. Rev. B* **61**, R13325 (2000).
- <sup>13</sup>C. Frontera, J. L. García-Muñoz, A. Llobet, and M. A. G. Aranda, *Phys. Rev. B* **65**, 180405 (2002).
- <sup>14</sup>M. Medarde, P. Lacorre, K. Conder, F. Fauth, and A. Furrer, *Phys. Rev. Lett.* **80**, 2397 (1998).
- <sup>15</sup>K. Conder, E. Pomjakushina, V. Pomjakushin, M. Stingaciu, S. Streule, and A. Podlesnyak, *J. Phys.: Condens. Matter* **17**, 5813 (2005).
- <sup>16</sup>P. Fischer, G. Frey, M. Koch, M. Könnicke, V. Pomjakushin, J. Schefer, R. Thut, N. Schlumpf, R. Bürge, U. Greuter, S. Bondt, and E. Berruyer, *Physica B* **276-278**, 146 (2000).
- <sup>17</sup>J. Rodríguez-Carvajal, *Physica B* **192**, 55 (1993).
- <sup>18</sup>T. Chatterji, F. Fauth, B. Ouladdiaf, P. Mandal, and B. Ghosh, *Phys. Rev. B* **68**, 052406 (2003).
- <sup>19</sup>J.-S. Zhou and J. B. Goodenough, *Phys. Rev. B* **60**, R15002 (1999).